Nigerian Journal of Technology (NIJOTECH)
Vol. 44, No. 4, December, 2025, pp. 567- 575
www.nijotech.com

Print ISSN: 0331-8443
Electronic ISSN: 2467-8821
https://doi.org/10.4314/njt.2025.5507

IMPACT OF WELDING CURRENT ON MICROSTRUCTURAL AND MECHANICAL CHARACTERISTICS OF CMT-WELDED 316L AUSTENITIC STAINLESS STEEL

AUTHORS:
D. Bhoyar*[1], N. Mungle[2], A. Band[3], G. Nagdeve[4], A. Mungle[5], and M. Muley[6]

AFFILIATIONS:
[1]PGTD Computer Science and Electronics, RTMNU Nagpur, INDIA.
[2]Department of Mechanical Engineering, Yeshawantrao Chavan College of Engineering, Nagpur, INDIA.
[3]Department of Data Science, Ramdeobaba University, Nagpur, INDIA.
[4]Department of Mechanical Engineering, Tulsiramji Gaikwad Patil College of Engineering & Technology, Nagpur, INDIA.
[5]Department of Pharmacy, Gurunanak College of Pharmacy, Nagpur, INDIA.
[6]Department of Mathematics, S B Jain Institute of Technology, Management and Research, Nagpur, INDIA.

***CORRESPONDING AUTHOR:**
Email: bhoyar.dipali@gmail.com

ARTICLE HISTORY:
Received: August 26, 2025.
Revised: November 27, 2025.
Accepted: November 28, 2025.
Published: January 03, 2026.

KEYWORDS:
316L Austenitic Stainless Steel (ASS), Cold Metal Transfer Welding, Welding Current, Dendritic Structures, Corrosion Resistance, Tensile Strength.

Abstract

316L Austenitic Stainless Steel (ASS) has an extensive demand in engineering applications including the chemical, petrochemical and nuclear sectors. These industries greatly benefit from the exceptional mechanical and corrosion-resistant qualities of 316L ASS welded joint. This study investigates 316L ASS welded joints using Cold Metal Transfer (CMT) welding with 100A, 110A and 120A welding currents at 11V constant voltage applying 309L filler material. The Base Metal (BM) exhibited majorly constant austenitic grains with increasingly higher current promoting the formation of wider Heat Affected Zone (HAZ), more dendritic 316L ASS weld microstructures which allows faster cooling rates; resulting in higher micro hardness, tensile strength and toughness. The result also showed that as the welding current increases from 100A to 120A the HAZ width increased from 26.2 µm to 50.6 µm. The highest hardness (173 HV) was observed at weld zone (WZ) of High Welding Current (HWC) weld joint as compared to Low Welding Current (LWC) and Medium Welding Current (MWC) weld joint with observed hardness of 150 HV and 167HV respectively. The HWC weld joint also exhibited higher tensile strength (665 MPa) as compared to LWC weld joint (597 MPa) and MWC weld joint (574 MPa). The toughness of MWC 45J) was found to be lowest as compared to LWC (66J) and HWC (128J) highest. With these higher mechanical properties due to favorable microstructure from different cooling rates, 316L ASS metal with weldments of 309L filler material is the most applicable material for higher corrosion resistant industrial designs.

ARTICLE INCLUDES:
Peer review

DATA AVAILABILITY:
On request from author(s)

EDITORS:
Chidozie Charles Nnaji

FUNDING:
None

1.0 INTRODUCTION

The chemical, petrochemical, and food production sectors rely on 300 series austenitic stainless steel (ASS) for its strong mechanical qualities and enhanced resistance to corrosion [1,2]. Around 60-70% industries use 300- series ASS due its nickel content which is very helpful for getting high mechanical properties [3]. Stainless Steel (SS) is presently employed in numerous types of industries such as marine, power plant, paper and pulp industries, nuclear power plants and automobile manufacturing industry [4]. Although stainless steel is costlier due to the presence of nickel in the composition. Its remarkable features, including impressive tensile strength and resistance to

HOW TO CITE:
Bhoyar, D., Mungle, N., Band, A., Nagdeve, G., Mungle, A., and Muley, M. "Impact of Welding Current on Microstructural and Mechanical Characteristics of CMT-welded 316l Austenitic Stainless Steel", *Nigerian Journal of Technology*, 2025. 44(4), pp. 567- 575. https://doi.org/10.4314/njt.2025.5507

corrosion, lead to a longer lifespan and lower cycle costs [5].

Presently there is a growing trend in industries to adopt the materials which have higher mechanical and corrosion characteristics which promotes financial growth [6,7]. Welding using arc-based techniques enables the connection of costly materials that possess favorable mechanical properties and resistance to corrosion [8]. This process ensures that the joint remains structurally sound and complies with the safety and strength requirements of the joint. Additionally, several industrial sectors such as nuclear industries, and gas and oil sectors need to achieve the necessary mechanical characteristics and corrosion resistance. This can be effectively managed by carefully selecting the right welding materials. Due to their exceptional blend of strength, corrosion resistance, weldability, durability, and ductility [9]. The most widely used grade is ASS. The ASS's weldability is decreased by thermal cracking that occurs during the welding process [10]. The occurrence of this flaw is attributed to fact that as disparity in linear expansion coefficient, melting point and thermal conductivity increases, so does the difficulty in achieving an equal weld strength between the metals [11]. To address these issues metallic fillers that correspond to materials to be joined cautiously selected.

Researchers reported that microstructural and mechanical properties improved due to the proper selection of fillers and having welding currents ranging from 80 to 190A with Cold Metal Transfer (CMT) welding [12,13]. They observed skeletal and lathy ferrite development due to ER309L filler [14]. Different heat inputs by CMT welded joints help to create δ-ferrite, which increases the mechanical characteristics (tensile strength) of the weld metal [15]. However, a number of studies have confirmed the mechanical and microstructural advantages of CMT welded joints. Detailed comparison of currents under identical parameters is not fully understood particularly with 316L ASS CMT weld metal joints. In the present investigation, systematic experimental investigation was carried out on 316L ASS welded joint with ER 309L fillers having welding currents (100, 110 and 120 A) with constant welding voltage to study the effect on the microstructural variations and its influence on the mechanical properties.

2.0 MATERIALS AND METHODS

2.1 Sample Preparation

316L ASS plates used in this experiment measured 120 x 75 x 3 mm^3 in length, width, and thickness respectively. For weld procedure, CMT welding was employed, utilizing a Fronius TPS 400i welding machine. The welding was performed in a single pass using an ER309L filler. Single butt joints were made with a root gap of 1.2 mm, and the welding process was carried out at three different currents (100 A, 110 A, and 120 A). In this paper, we have considered 100 A as low welding current (LWC), 110 A as medium welding current (MWC) and 120 A as high welding current (HWC). To guarantee adequate shielding during the welding process, argon gas was utilized as the shielding gas, and the flow rate was kept at 10 lit/min [16]. This setup ensured effective welding with minimal oxidation and defects, providing a clean and strong joint. Figure 1 shows the welded plates with different welding currents.

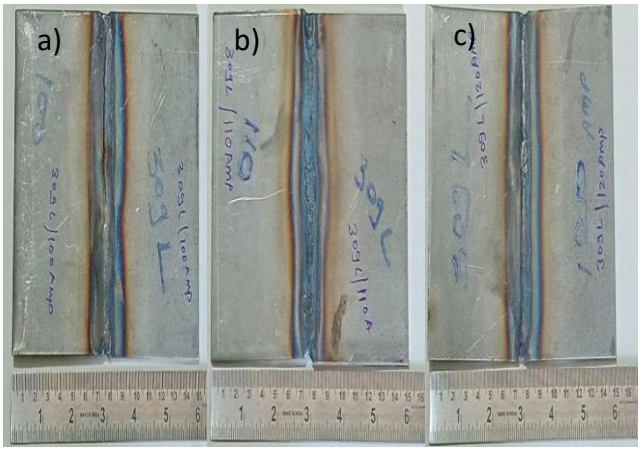

Figure 1: Welded plates with **a**) LWC **b**) MWC and **c**) HWC

Table 1 provides the chemical composition of both the base material (BM) and the fillers, expressed in weight percentages [17]. To prepare the various samples required for mechanical testing and other evaluations, wire-cut EDM 520 NXG PRO 1 were used. In **Table 2**, the welding parameters for different current levels were presented, which are categorized as Low Welding Current (LWC), Medium Welding Current (MWC), and High Welding Current (HWC). The heat input (HI) for each welding condition was calculated using equation (1). The selection of welding current is critical in influencing the thermal profile and quality of the weld, which impacts the overall mechanical qualities and performance of the welded connection. This approach ensures that the samples are prepared

https://doi.org/10.4314/njt.2025.5507

under controlled conditions, allowing for consistent and reliable testing results.

$$HI = \eta \frac{V*I}{s} \; KJ/mm \quad (1)$$

Where, I- welding current in amperes (A), *s*- welding speed in mm/s, V- voltage in volts (V), and η- efficiency of GTAW as 0.7 [18].

Table 1: Base metal and filler chemical composition in wt%

Materials	C	Si	Mn	P	S	Cr	Mo	Ni	N	Co	Cu	Fe
AISI 316L ASS	0.018	0.440	1.339	0.031	0.003	16.926	2.172	10.044	0.002	-	-	Bal
ER 309L Filler	0.03	0.4	1.5	0.03	0.03	24.0	0.75	13.0	4.0	-	-	Bal

Table 2: Welding variables in various welding currents

Specimens	Welding Speed (*s*) (mm/s)	Current (A)	Voltage (V)	Heat input (KJ/mm)
LWC	1.09	100	11	0.7064
MWC	1.56	110	11	0.5429
HWC	1.79	120	11	0.5162

2.2 Microstructural Properties

After welding, samples were sectioned into 10 x 10 x 3 mm^3 dimensions to facilitate microstructural analysis. Silicon carbide abrasive sheets were used to polish the samples thoroughly with grit sizes of 200, 400, 800, 1200, 1500, 2000, and 2500 to obtain a smooth surface for observation. To distinguish between the BM and weld metal (WM), the polished specimens were exposed to a marble's reagent for 5 seconds [19]. The microstructures of various welded regions were closely examined using a Scanning Electron Microscope (SEM) JEOL JSM G3DQA. Additionally, Energy Dispersive Spectroscopy (EDS) was employed in conjunction with the SEM to analyze the elemental composition and determine the weight percentages of the various elements present. To further investigate the phases within the weld zone, X-ray Diffraction (XRD) analysis was performed. This combination of techniques enables a full understanding of the welded specimen's microstructural features, elemental distribution, and phase identification, all of which are crucial for defining the quality and functionality of the welded joints.

2.3 Mechanical Properties

The Truemet testing machine was used to apply 500 gf of steady load for 10 seconds to test Vicker's hardness. ASTM E92 standard was used for microhardness testing [20]. The universal testing machine (UTM) UTS HGFL-TS was utilized for testing the tensile sample. The sample was prepared using ASTM E8 standard [21]. The gauge length, thickness and width were 30, 3 and 10 mm respectively. The crosshead speed was taken as 20mm/min. The V-notch Charpy Impact test was carried out at room temperature on a sample measuring 55 mm in length, 10 mm in width, and 3 mm in thickness, with a 45^0 notch of 2 mm. ASTM E23 standard were used for testing the toughness for the samples [22]. To check the repeatability, all mechanical tests were repeated and the average mechanical properties were measured.

3.0 RESULTS AND DISCUSSION

3.1 Microstructural Analysis

Figure 2 presents scanning electron microscope (SEM) images of different zones—BM, HAZ , fusion zone (FZ), and WZ—produced by Cold Metal Transfer Welding at different welding currents. The SEM analysis of the 316L ASS BM primarily reveals an austenitic phase, which is observed as the white regions in the images. The welding process causes these zones to exhibit distinct microstructural features. This is mainly due to the welding with limited thermal diffusion [23]. As the welding current increases, so does the HAZ. The width of the HAZ was depicted in Table 3. The HAZ is wider in HWC weld joints than in MWC and LWC. This data shows that when welding current increases, the width of the HAZ increases as well. An increase in welding current decreases heat input, improving cooling rate. The higher cooling rate results in extended heat retention,

https://doi.org/10.4314/njt.2025.5507

promoting grain growth and consequently increasing the HAZ width [24]. In weld zone, the dendritic regions are mainly composed of columnar/equiaxed dendrites, which is mainly due to solidification or temperature differences across the welded joint.

Table 3: HAZ measurement for varying welding currents in µm

Sample No.	Specimens	HAZ (µm)
1	LWC	26.2
2	MWC	32.7
3	HWC	50.6

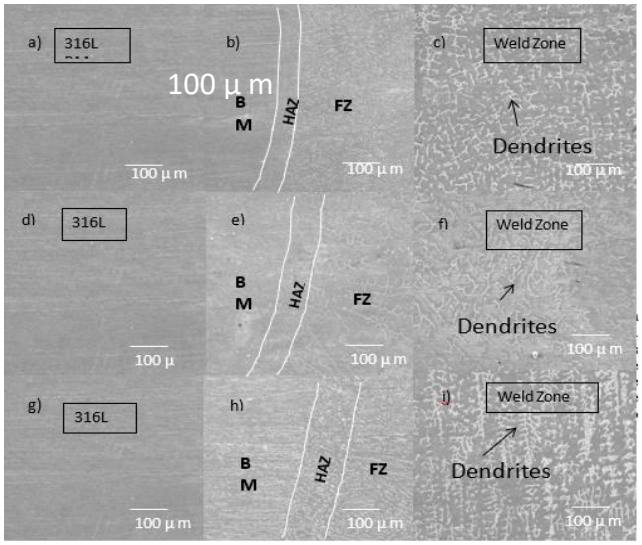

Figure 2: Scanning electron microscope (SEM) images of (**a**) 316L BM for LWC, (**b**) Interface zone for LWC, (**c**) Weld zone for LWC, (**d**) 316L BM for MWC, (**e**) Interface zone for MWC, (**f**) Weld zone for MWC, (**g**) 316L BM for HWC, (**h**) Interface zone for HWC and (**i**) Weld zone for HWC

Figure 3 shows XRD analysis of 316L BM having mainly austenite peaks, however, variations in peak intensity were observed and no other intermetallic compounds were detected in the BM. Conversely, the dendritic structures were observed in three distinct welds near the fusion boundary, as demonstrated in Fig. 2 (c, f, i), as a result of the increased cooling rate [25]. Ferrite and austenite phases make up the majority of the WM structures in all three welds. However, in LWC, the austenite phase is prevalent and distinguishable from other welds. This feature was mainly developed due to the post-solidification cooling transformation [26]. The $Cr_{23}C_6$ (Chromium Carbide) phase were also observed in three different welds which was confirmed by the EDS point scan analysis.

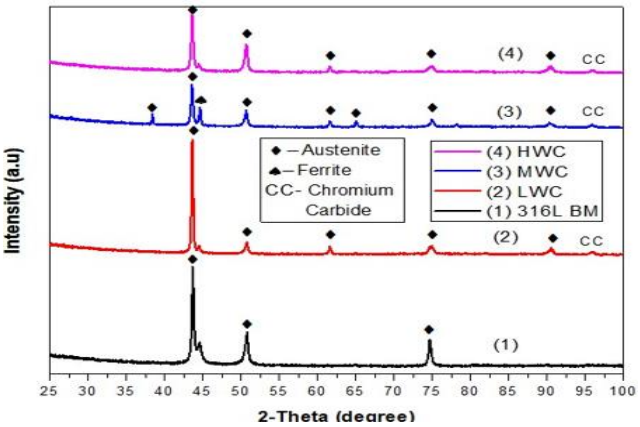

Figure 3: XRD analysis of 316L BM and LWC welds

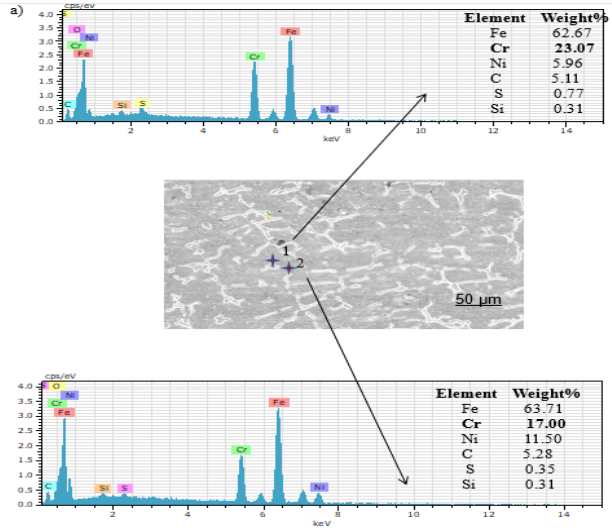

Figure 4a: SEM micrographs of LWC along with EDS analysis

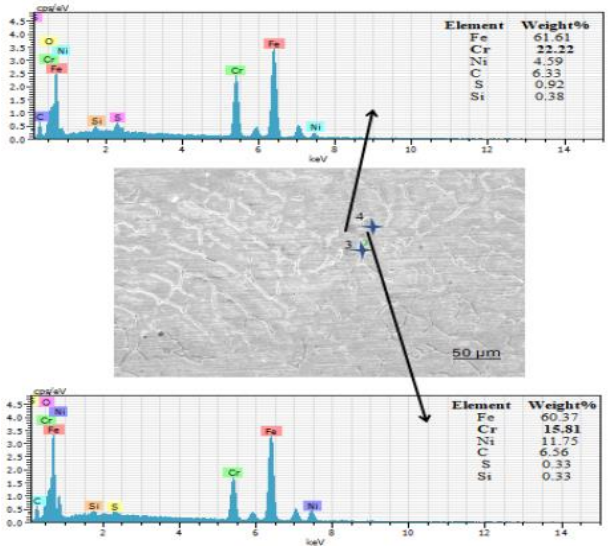

Figure 4b: SEM micrographs of MWC along with EDS analysis

https://doi.org/10.4314/njt.2025.5507
http://creativecommons.org/licenses/by-nc-nd/4.0/

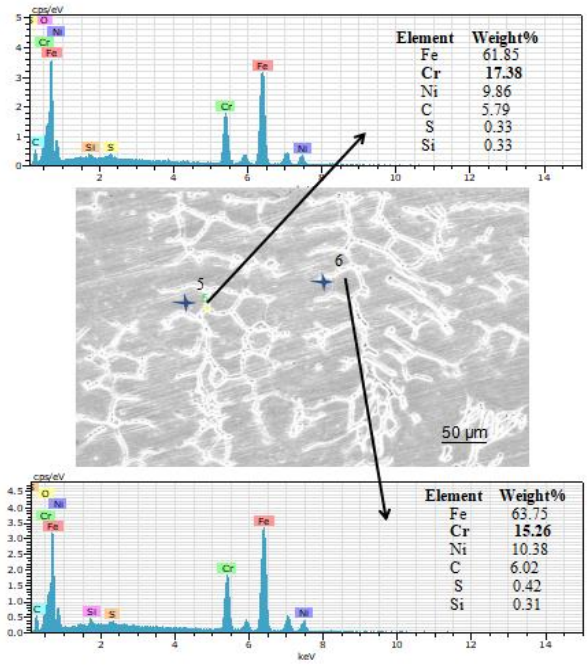

Figure 4b:SEM micrographs of HWC along with EDS analysis

3.2 Micro-hardness Test

Figure 5 illustrates the bar chart representing the hardness test of the weld cross-section conducted on 316L BM, HAZ, and WZ. Five readings were taken, and averages are reported for each region (BM, HAZ, and WZ) of the specimen. The average hardness at 316L BM is 163 HV, 158 HV and 161 HV for LWC, MWC and HWC respectively. The hardness decreases from HAZ for LWC (avg.165 HV) to MWC (avg.154 HV) and increases for HWC (avg.168 HV).

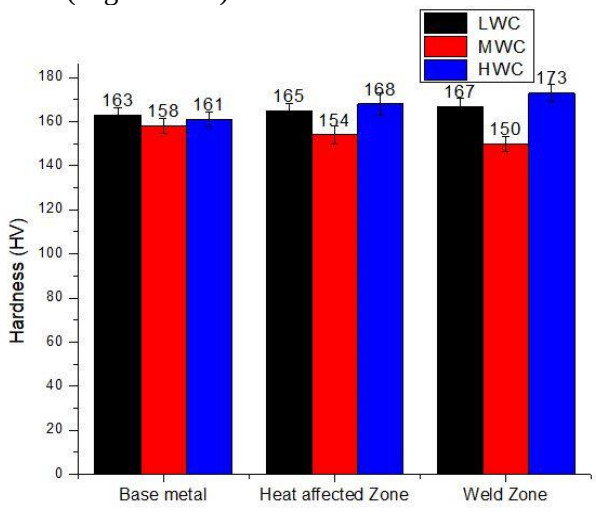

Figure 5: Microhardness results across various zones for LWC, MWC and HWC joint

Moreover, in the weld zone, the hardness for HWC (avg.173 HV) found higher as compared to MWC (avg.150 HV) and LWC (avg.167 HV) joint. The higher welding current, accompanied by the faster cooling rate, stimulates the production of dendritic structure, which increases the hardness of the weld [28]. A significant rise in the microhardness profile of the HAZ was also discovered, presumably due to the presence of partially un-melted grains near the FZ [29]. The average error for BM, HAZ and WZ is taken as $\pm$ 3.5, $\pm$ 4 and $\pm$ 5 for LWC, MWC and HWC specimen respectively.

3.3 Tensile Test

Figures 6 a) and 6 b) shows the specimen before and after fracture, respectively. The weld joint shows significant plastic deformation before fracture occurs [30]. The maximum tensile strength (~665 MPa) was observed for HWC weld joint followed by (~597 MPa) for LWC and (~574 MPa) for MWC weld. HWC exhibited the highest tensile strength when compared to LWC and MWC welds. This may be due to the finer morphology of the dendrites in the FZ and relatively high dendritic structure content [31]. In the tensile test, all three specimens fractured at the fusion zone (FZ), primarily in the HAZ, as illustrated in figure 6 c) in red colour. The failure at this juncture may be attributed to precipitates like $Cr_{23}C_6$ (see fig.3), which diminish ductility and induce fracture at this location. The tensile strength, yield strength and percentage elongation for 316L BM are ~608 MPa, ~358 MPa and 52 % respectively. The tensile strength, yield strength and percentage elongation for HWC weld specimen was found to be greater than 316L BM. Figure 7 a) shows the tensile stress-strain curve for the specimen and Fig.7 b) depicts the bar graph for tensile strength (TS) and yield strength (YS) with standard error of $\pm$ 9, $\pm$ 8 and $\pm$ 10 for LWC, MWC and HWC respectively. Fig.7 c) shows the percentage elongation and reduction in area of the specimen with standard error $\pm$ 1.2, $\pm$ 0.8 and $\pm$ 1.0 for LWC, MWC and HWC respectively. The percentage elongation of LWC, MWC and HWC are 49, 44 and 51%. Reduction in area decreased for MWC (59%) as compared to LWC (70%) and HWC (65%). The ductility of 316L ASS weld specimens can be affected by variety of parameters, including alloying elements, internal stress, and dislocation density [32,33]. From results it was found that, HWC weld joint has higher tensile/yield strength and reduced ductility than 316L ASS BM.

https://doi.org/10.4314/njt.2025.5507

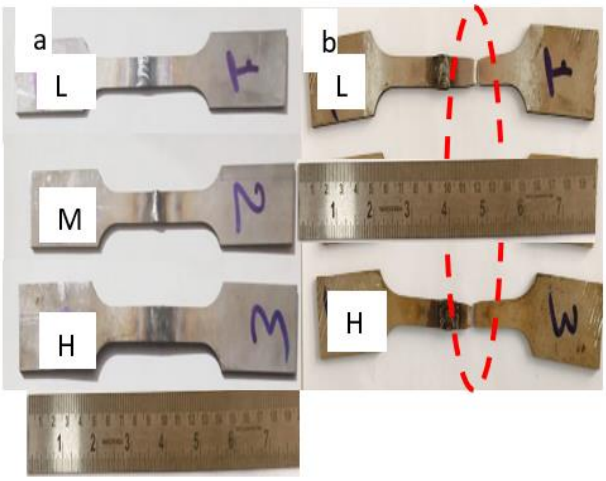

Figure 6: Tensile specimen of LWC, MWC and HWC welds a) before fracture and b) after fracture

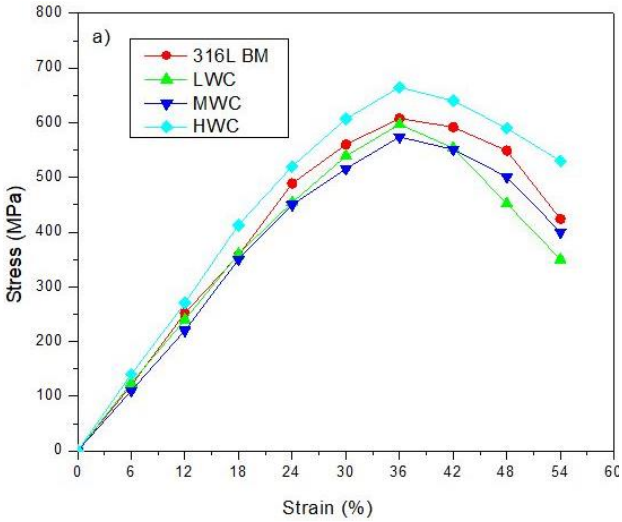

Figure 7a: Stress strain diagram of BM, LWC, MWC and HWC weld specimens

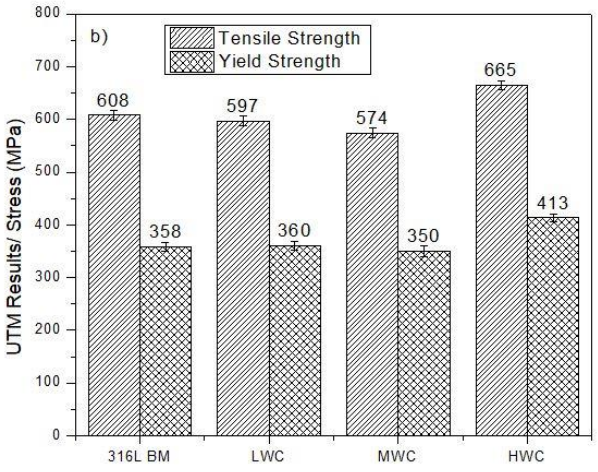

Figure 7b: Tensile Strength of BM, LWC, MWC and HWC weld specimens

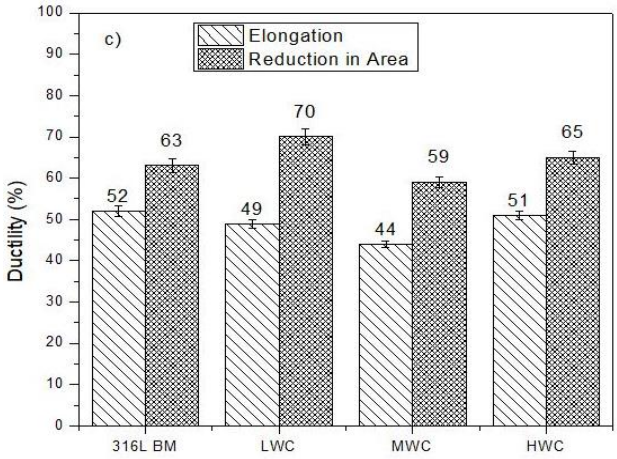

Figure 7c: Ductility of BM, LWC, MWC and HWC weld specimens

3.4 Impact Test

Impact toughness values for 316L ASS BM were found to be ~49J. The highest impact toughness was observed for HWC weld (~ 128 J). On the contrary, LWC weld exhibits an impact energy of (~ 66 J), as compared to MWC weld (~45 J) as shown in Fig.8. The high Nickel content causes dendritic structures, notably δ-ferrite, to form during the HWC weld process. The cooling rate and heat input significantly affect δ-ferrite content. Increased heat input decreases the formation of δ-ferrite in the microstructure by slowing cooling rates [34]. Therefore, in LWC weld the toughness values are less as compared to MWC and HWC weld.

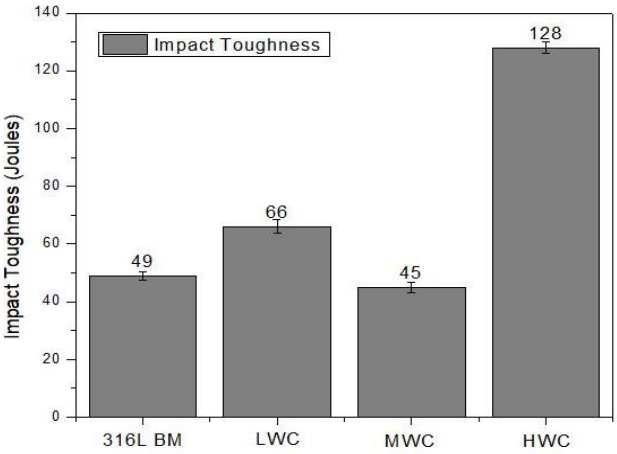

Figure 8: Impact toughness for 316L BM, LWC, MWC and HWC weld

4.0 CONCLUSIONS

The 316L ASS was successfully welded by Cold Metal Transfer Welding with ER309L filler with different welding currents. The following conclusions were derived from this investigation.

https://doi.org/10.4314/njt.2025.5507
http://creativecommons.org/licenses/by-nc-nd/4.0/

1) As the welding current increases, dendritic areas arise, as seen by the microstructural analysis of weldments.

2) The increase in welding current increases the growth of dendritic structures, notably δ-ferrite, which leads to higher mechanical properties.

3) The average hardness of HWC (avg.173 HV) is highest as compared to LWC (avg.167 HV) and MWC (avg.150 HV) due to the increase in cooling rate.

4) HWC (~665 MPa) has the highest tensile strength, followed by LWC (~597 MPa) and MWC (~ 574 MPa). The high welding current procedure reduces heat input, resulting in a larger heat affected zone due to increased cooling rate and creation of δ-ferrite, which increases tensile strength.

5) The toughness of MWC (~ 45J) was found to be lowest as compared to LWC (~66 J) and HWC (~ 128J). This is primarily due to slower cooling rates induced by hardness variations.

REFERENCES

[1] Kaladhar, M. Subbaiah, K. V. and Rao, C. S. "Machining of Austenitic Stainless Steels–a review," *International Journal of Machining and Machinability of Materials*, 12(1-2), p. 178-192, 2012. https://doi.org/10.1504/IJMMM.2012.048564

[2] Ambade, S. Patil, A. P. Tembhurkar, C. K.and Meshram, D. B. "Effect of Filler and Autogenous Welding on Microstructure, Mechanical and Corrosion Properties of Low Nickel Cr-Mn ASS". Advances in Materials and Processing Technologies, 8(3), p. 3454-3469, 2021. https://doi.org/10.1080/2374068X.2021.1970989

[3] Rajesh, K. D. Buddi, T. Kanth, P. R. and Satyanarayana, K. "Microstructural and Corrosion Resistance Study on Plasma Arc Welded Joints of AISI 304 and AISI 316". *Advances in Materials and Processing Technologies*, 6(2), p. 189-205, 2020. https://doi.org/10.1080/2374068X.2020.1732158

[4] Boillot, P. and Peultier, J. "Use of StainlessSteels in the Industry: Recent and Future Developments". *Procedia Engineering*, 83, p. 309-321, 2014. https://doi.org/10.1016/j.proeng.2014.09.015

[5] Francis, R. and Byrne, G. "Duplex Stainless Steels—Alloys for the 21st century". *Metals*, 11(5), p. 836, 2021. https://doi.org/10.3390/met11050836

[6] Milosev, I. and Scully, J. R. "Challenges for the Corrosion Science, Engineering, and Technology Community as a Consequence of Growing Demand and Consumption of Materials: A Sustainability Issue". *Corrosion*, 79(9), p. 988-996, 2023. https://doi.org/10.5006/4428

[7] Bender, R. Feron, D. Mills, D. Ritter, S. Babler, R. Bettge, D. and Zheludkevich, M. "Corrosion Challenges towards a Sustainable Society", *Materials and corrosion*, 73(11), p. 1730-1751, 2022. https://doi.org/10.1002/maco.202213140

[8] Khoshnaw, F. Krivtsun, I. and Korzhyk, V. "Arc Welding Methods", *Welding of metallic materials*, p. 37-71, 2023. https://doi.org/10.1016/B978-0-323-90552-7.00004-3

[9] Montemor, M. F. "Corrosion Issues in Joining Lightweight Materials: A review of the latest achievements", *Physical Sciences Reviews*, 1(2), 20150011, 2016. https://doi/10.1515/psr-2015-0011

[10] Bansod, A. V. Patil, A. P. and Shukla, S. "Effect of Heat on Microstructural, Mechanical and Electrochemical Evaluation of Tungsten Inert Gas Welding of Low-Nickel ASS". *Anti-Corrosion Methods and Materials*, 65(6), p.605-615, 2018. https://doi.org/10.1108/ACMM-05-2018-1941

[11] Armentani, E. Esposito, R. and Sepe, R. "The Effect of Thermal Properties and Weld Efficiency on Residual Stresses in Welding", *Journal of achievements in materials and manufacturing engineering*, 20(1-2), p. 319-322, 2007.

[12] Tang, Y. Ye, X. Ding, L. Zhang, P. Yu, Z. and Wu, D. "Microstructures and Mechanical Properties of Ni/Fe Dissimilar Butt Joint Welded Using the Cold Metal Transfer", *Materials Research Express*, 7(4), 046516,

2020.https://doi.org/10.1088/2053-1591/ab8843

[13] Varghese, P. Vetrivendan, E. Dash, M. K. Ningshen, S. Kamaraj, M. and Mudali, U. K. "Weld Overlay Coating of Inconel 617 M on Type 316 L Stainless Steel by Cold Metal Transfer Process", *Surface and Coatings Technology*, 357, p. 1004-1013, 2019. https://doi.org/10.1016/j.surfcoat.2018.10.073

[14] Verma, J. Taiwade, R. V. Khatirkar, R. K. and Kumar, A. "A Comparative Study on the Effect of Electrode on Microstructure and Mechanical Properties of Dissimilar Welds of 2205 Austeno-Ferritic and 316L Austenitic Stainless Steel", *Materials Transactions*, 57(4), p. 494-500, 2016. https://doi.org/10.2320/matertrans.M2015321

[15] Kannan, A. R. Shanmugam, N. S. and Vendan, S. A. "Effect of Cold Metal Transfer Process Parameters on Microstructural Evolution and Mechanical Properties of AISI 316L Tailor Welded Blanks", *The International Journal of Advanced Manufacturing Technology*, 103, p. 4265-4282, 2019. https://doi.org/10.1007/s00170-019-03856-2

[16] Ambade, S. Tembhurkar, C. Rokde, A. Gupta, S. Shelare, S. Prakash, C. Gupta, L. R. and Smirnov,V. A. "Experimental Investigation of Microstructural, Mechanical and Corrosion Properties of 316L and 202 Austenitic Stainless-Steel Joints using Cold Metal Transfer Welding", *Journal of Materials Research and Technology*, 27, p. 5881-5888, 2023. https://doi.org/10.1016/j.jmrt.2023.11.091

[17] Tembhurkar, C. Ambade, S. Kataria, R. Verma, J. Moon, A. "Cold Metal Transfer Welding of 316L/430 Dissimilar Stainless-Steel Welds", *Anti-Corrosion Methods and Materials*, 72(2), 178-188,2025. https://doi.org/10.1108/ACMM-03-2023-2774

[18] Shanmugasundar,G. Bansod, A. Schindlerova, V. and Cep, R. "Influence of Filler Material on the Microstructural and Mechanical Properties of 430 Ferritic Stainless Steel Weld Joints". *Materials*, 16(4), p. 1590, 2023. https://doi.org/10.3390/ma16041590

[19] Nanavati P. K. "Studies on Effect of Welding Parameters on Corrosion and Mechanical Behaviour of Duplex Stainless-Steel Welds" (Doctoral dissertation, Maharaja Sayajirao University of Baroda (India), 2018.

[20] Chohan, I. M. Ahmad, A. Sallih, N. Bheel, N. Salilew,W. M. and Almaliki, A. H. "Effect of Seawater Salinity, pH, and Temperature on External Corrosion Behavior and Microhardness of Offshore Oil and Gas Pipeline: RSM Modelling and Optimization", *Scientific Reports*, 14(1), 16543, 2024. https://doi.org/10.1038/s41598-024-67463-2

[21] Kashaev, N. Horstmann, M. Ventzke, Riekehr, V. S. and Huber, N. "Comparative Study of Mechanical Properties Using Standard and Micro-specimens of Base Materials Inconel 625, Inconel 718 and Ti-6Al-4áV", *Journal of materials research and technology*, 2(1), p. 43-47, 2013. https://doi.org/10.1016/j.jmrt.2013.03.003

[22] Srivastava, K. Sinha, A. A. and Sahani, R. "Effect of Heat Treatment on Hardness and Toughness of EN8 steel", *Materials Today: Proceedings*, 42, p. 1297-1303, 2021. https://doi.org/10.1016/j.matpr.2020.12.1015

[23] Kumar, N. Kumar, P. and Pandey, C. "Influence of Filler Materials on GTAW Dissimilar Welds: Inconel 718 and Austenitic Stainless Steel 304L", *Archives of Civil and Mechanical Engineering*, 24(4), 231, 2024. https://doi.org/10.1007/s43452-024-01042-0

[24] Shrivastava, R. Kumar, R. R. Santhoshkumar, R. Anoop, C. R. Cyriac, J. Chakravarthy,P. and Murty, S. N. "Effect of Grain Size on the Heat-Affected Zone (HAZ) Cracking Susceptibility in Ni Base XH67 Superalloy", *Metallurgical and Materials Transactions A*, 55(1), p. 183-197, 2024. https://doi.org/10.1007/s11661-023-07241-3

[25] Zhang ,X. Ji, M. Xu,L. and Chu, Y. "Effect of Dendritic Structure and Secondary Phases on the Fatigue Behaviour of ERNiCrMo-3 Weld Metal", *International Journal of Fatigue*, 180, 108113, 2024.

https://doi.org/10.1016/j.ijfatigue.2023.108113

[26] Zhao, R. Kou, R. Wang, H. Song,C. Li, C. and Sun, Z. "The Effects of Specimens Geometry on Solidification Conditions and Microstructure Formation in Laser Powder Bed Fusion Fabricated Ti–6Al–4V alloys", *Journal of Materials Research and Technology*, 33, p. 5030-5039, 2024. https://doi.org/10.1016/j.jmrt.2024.10.095

[27] Ranjbar, K. Dehmolaei, R. Amra, M. and Keivanrad, I. "Microstructure and Properties of a Dissimilar Weld Between Alloy 617 and A387 Steel using Different Filler Metals", *Welding in the World*, 62, p. 1121-1136, 2018. https://doi.org/10.1007/s40194-018-0610-x

[28] Holovko , V. V. Yermolenko, D. Y. and Stepanyuk,S. M. "The Influence of Introducing Refractory Compounds into the Weld Pool on the Weld Metal Dendritic Structure", *The Paton Welding Journal*, 6, p. 2-8, 2020. https://doi.org/10.37434/tpwj.

[29] Vashishtha, H. Taiwade, R. V. Sharma , S. and Marodkar, A. S. "Microstructural and Mechanical Properties Evolution of Bimetallic Cr-Ni and Cr-Mn-Ni stainless SteelJoints", *Metallography, Microstructure, and Analysis*, 8, p. 359-369, 2019. https://doi.org/10.1007/s13632-019-00549-w

[30] Cooper, D. R. and Allwood, J. M. "The Influence of Deformation Conditions in Solid-State Aluminium Welding Processes on the Resulting Weld Strength", *Journal of Materials Processing Technology*, 214(11), p. 2576-2592, 2014. https://doi.org/10.1016/j.jmatprotec.2014.04.018

[31] Sonar, T. Balasubramanian,V. Malarvizhi,S. Venkateswaran, T. and Sivakumar,D. "An Overview on Welding of Inconel 718 Alloy-Effect of Welding Processes on Microstructural Evolution and Mechanical Properties of Joints", *Materials Characterization*, 174, 110997, 2021. https://doi.org/10.1016/j.matchar.2021.110997

[32] Kumar, T. S. Yadav, S. D. Nagesha, Kannan, A. R. and Reddy, G. P. "Isothermal and thermomechanical fatigue behaviour of type 316LN austenitic stainless steel base metal and weld joint", *Materials Science and Engineering: A*, 772, 138627, 2020. https://doi.org/10.1016/j.msea.2019.138627

[33] Zhou , X. Liu,Y. Qiao, Z. Guo, Q. Liu,C. Yu, L. and Li, H. "Effects of Cooling Rates on δ-ferrite/γ-Austenite Formation and Martensitic Transformation in Modified Ferritic Heat-Resistant Steel", *Fusion Engineering and Design*, 125, p. 354-360, 2017. https://doi.org/10.1016/j.fusengdes.2017.05.095

[34] Ni,Z. L. Liu,Y. Wang, Y. H. and He, B. Y. "Interfacial Bonding Mechanism and Fracture Behaviour in Ultrasonic Spot Welding of Copper Sheets", *Materials Science and Engineering: A*, 833, 142536, 2022. https://doi.org/10.1016/j.msea.2021.142536